



## Future trends in the vertical structure of Arctic warming and moistening in different emission scenarios

Hanbin Nie <sup>a,b</sup>, Yongkun Xie <sup>a,\*</sup>, Min Zhao <sup>a,b</sup>, Zifan Su <sup>a,b</sup>

<sup>a</sup> Collaborative Innovation Center for Western Ecological Safety, Lanzhou University, Lanzhou 730000, China

<sup>b</sup> College of Atmospheric Sciences, Lanzhou University, Lanzhou 730000, China

### ARTICLE INFO

**Keywords:**

Arctic warming  
Arctic moistening  
Vertical structure  
Future scenarios

### ABSTRACT

Arctic warming is a pressing global concern, and understanding its future vertical structure is crucial for Arctic–mid-latitude connections. In this study, we employed the Coupled Model Intercomparison Project Phase 6 (CMIP6) multi-model simulations to investigate the vertical structure of Arctic warming concerning its current evolving (1980–2030) and future change (2050–2100). In addition to the dry atmosphere described only by temperature, this study analyzed humidity and moist static energy (MSE) for the moist (with the effect of moisture explicitly presented) atmosphere. Under the high-emission scenario, Arctic warming is projected to accelerate, while maintaining its existing bottom-heavy structure. Amplified humidity increases are anticipated in both the tropics and the Arctic, with the Arctic exhibiting greater moisture increases in percentage. Furthermore, we find that MSE, serving as a comprehensive metric for moist atmospheric warming, is projected to accelerate in the Arctic under the high-emission scenario. As a result, the warming of both the dry and moist atmospheres will intensify in the future, with the bottom-heavy vertical structure persisting due to enhanced warming and moistening in the lower troposphere. The accelerated Arctic moistening in the future is due to meridional atmospheric moisture transport in the summer and local moisture source in the winter. In contrast, under the intermediate-emission scenario, Arctic warming and moistening are not projected to accelerate. Despite the inter-model discrepancy, our findings underscore the reliability of projections derived from the high-emission scenario. In summary, our findings highlight that the bottom-heavy vertical structure of Arctic warming will not change and that enhanced upper-level Arctic warming will not occur in the future.

### 1. Introduction

Amplified Arctic warming has garnered worldwide attention in recent decades because of its geographical particularity, extreme magnitude, and potential influence on other regions (Serreze and Barry, 2011; Francis and Vavrus, 2012; Li and Wu, 2012; Cohen et al., 2019; Gulev et al., 2021; You et al., 2021; Zhang et al., 2022; Yin et al., 2023). The Arctic has experienced the strongest warming on Earth, with surface temperatures rising nearly four times the global average since 1979 (Huang et al., 2017; Cai et al., 2021; Rantanen et al., 2022). It is suggested that Arctic warming is related to anthropogenic greenhouse gas emissions (Xie et al., 2019; Gulev et al., 2021), retreating sea ice/snow cover and corresponding albedo reduction (Screen et al., 2012; Overland and Wang, 2013; Dai et al., 2019; Kim et al., 2019; Hahn et al., 2022; Xie et al., 2022a), feedbacks associated with longwave radiation and moisture (Lu and Cai, 2009; Pithan and Mauritsen, 2014; Gao et al., 2019; Cai

et al., 2022), and atmospheric and oceanic heat transport (Cai, 2005; Graversen et al., 2008; Delworth et al., 2016; Tsubouchi et al., 2021; Xie et al., 2023a). It is suggested that the warming-induced retreat of sea ice could lead to alterations in atmospheric circulation and climate patterns across different seasons (Deser et al., 2010; Screen and Simmonds, 2010; Boeke and Taylor, 2018; Ding et al., 2021). In addition, it is suggested that Arctic warming influences the mid-latitude climate by affecting the subtropical jet stream (Barnes and Polvani, 2015; Wu et al., 2016; He et al., 2020), Siberian High (Nakamura et al., 2015; Labe et al., 2020; Papritz, 2020), Ural blocking (Luo et al., 2019; Peings, 2019), stationary wave trains and potential vorticity advection (Xie et al., 2020, 2023b; Duan et al., 2022), and multisphere interactions (Xie et al., 2022b). In turn, the Arctic temperature and sea ice can also be influenced by the lower latitudes through atmospheric and oceanic circulations (Wu et al., 2006, 2013; Wu, 2017; Polyakov et al., 2023; Wu and Ding, 2023). The Arctic climate change is projected to persist in the future; for example,

\* Corresponding author.

E-mail address: [xieyk@lzu.edu.cn](mailto:xieyk@lzu.edu.cn) (Y. Xie).

the Arctic could be ice-free in summer by the 2030s (Overland and Wang, 2013; Notz and Stroeve, 2018; Docquier and Koenigk, 2021; Xie et al., 2022a).

The vertical structure of Arctic warming is suggested to be crucial for mid-latitude atmospheric circulation responses (He et al., 2020; Labe et al., 2020; Xie et al., 2020; Kim et al., 2021). Although a middle-heavy structure (the magnitudes are larger at the middle level) was suggested for Arctic warming (Graversen et al., 2008), updated data reveals that Arctic warming is characterized by a bottom-heavy structure, that is, larger anomalies are trapped at the bottom (Screen and Simmonds, 2010). Different vertical structures of Arctic warming have different effects on atmospheric circulation and temperature patterns (Kim et al., 2021; Xie et al., 2022b). Relative to a surface-trapped or bottom-heavy profile, stronger upper-level Arctic heating can provoke stronger circulation anomalies in the mid-latitudes (Kim et al., 2021). In addition to the vertical structure, a larger magnitude of bottom-heavy Arctic warming could also have a greater influence on mid-latitude circulation (Xie et al., 2022b). The potential vorticity dynamics indicate that the atmospheric circulation response to the diabatic heating depends on the vertical structure and magnitude of the diabatic heating (Hoskins et al., 1985; Wu et al., 2020), which explains why the mid-latitude response varies with varied vertical structure or magnitude of Arctic warming (Xie et al., 2020, 2023b). Therefore, the vertical structure of Arctic warming is crucial for its influence on weather and climate in remote regions. The investigation of the vertical structure of Arctic warming holds great significance, not only for the Arctic itself but also for its interconnected relationships with mid-latitudes, necessitating a thorough examination of its future changes.

Aside from temperature, humidity and precipitation are also significant aspects to consider when discussing climate change in a moist atmosphere. Because of hydrological cycle changes (Held and Soden, 2006), latent heat associated with the phase transition of water is of significance to global warming (Matthews et al., 2022; Song et al., 2022). Changes in the Arctic water cycle, such as increases in atmospheric moisture and evaporation during winter, have been observed (Lu and Cai, 2009; Vihma et al., 2016). It is suggested that atmospheric moisture transport is crucial for the moisture increase, that is, Arctic moistening (Graversen et al., 2008; Gao et al., 2019; Cai et al., 2022, 2024). Atmospheric moisture transport is modulated by factors including North Atlantic storm tracks (Zhang et al., 2008, 2013), El Niño–Southern Oscillation (Luo et al., 2023), atmospheric rivers (Zhang et al., 2023), and enhanced warming over the Tibetan Plateau and Asian dryland (Xie et al., 2023a). Nonetheless, the vertical structure of Arctic moistening has not been sufficiently investigated. Therefore, for the practical moist atmosphere, this study also investigated the changes in the vertical structure of humidity and moist static energy (MSE). Analogous to equivalent temperature and equivalent potential temperature (Matthews et al., 2022; Song et al., 2022), MSE explicitly accounts for the impact of latent heat change on the energy and temperature of the moist atmosphere.

The review above indicates that there is still uncertainty regarding the future changes in the vertical structure of Arctic warming and moistening. This study undertook a thorough analysis of the changes in the vertical structure of Arctic warming and moistening during present and future time periods in order to address this topic. This paper is organized as follows: Section 2 provides detailed descriptions of the data and methods. Section 3 presents the trends of temperature, humidity, and MSE in the present and future. Section 3 also compares the changes in the vertical structure of the Arctic climate under two emission scenarios. The mechanisms behind the projected increase in Arctic humidity are described in Section 3.4. Section 4 summarizes the key findings of this study.

## 2. Data and methods

### 2.1. CMIP6 simulations

The simulations from thirty-one models (Table S1) that participated in the Coupled Model Intercomparison Project Phase 6 (CMIP6; Eyring et al., 2016) were examined in this study. The historical experiment and Shared Socioeconomic Pathways (SSP)-based high-emission and intermediate-emission future scenarios, SSP5–8.5 and SSP2–4.5, were examined (Eyring et al., 2016; O'Neill et al., 2017). SSP5–8.5 is characterized by a high radiative forcing trajectory, primarily due to the increased concentration of greenhouse gases (GHGs) such as carbon dioxide, methane, and nitrous oxide. In this scenario, GHG emissions continue to rise throughout the 21st century, resulting in a substantially warmer climate. In contrast, SSP2–4.5 represents an intermediate-emission pathway with a more moderate increase in GHG concentrations. Emissions in SSP2–4.5 peak around the mid-21st century and then gradually decline, leading to a lower radiative forcing and a less extreme warming trajectory. The examined variables are listed in Table S2. All models with the required variables were used.

The CMIP6 historical and SSP5–8.5 or SSP2–4.5 experiments cover the periods from 1850 to 2014 and from 2015 to 2100, respectively. For our analysis, a half-century period from 1980 to 2030 was chosen to reflect current climate change, whereas another half-century period from 2050 to 2100 was considered to represent future change. The 1980–2030 time series includes two periods: 1980–2014 from the historical experiment and 2015–2030 from the SSP5–8.5 and SSP2–4.5 experiments. When more than three ensemble members were available, only the first three ensemble members were used for convenience (Table S1). Before calculating the mean of the multi-model ensemble, the ensemble members of each model were averaged. To plot the mean results of the multi-mode ensemble, the model outputs were bilinearly interpolated onto a  $1.0^\circ \times 1.0^\circ$  horizontal grid. The four boreal seasons are defined as follows: spring, from March to May; summer, from June to August; autumn, from September to November; and winter, from December to the following February.

### 2.2. Reanalysis data

The fifth-generation ECMWF reanalysis dataset (ERA5; Hersbach et al., 2020) was used for comparison with the CMIP6 simulations. ERA5 is the latest version of the ECMWF reanalysis and is available for the period ranging from January 1940 to the present, wherein pressure-level data were used. ERA5 data are in the monthly mean and have a resolution of  $1^\circ \times 1^\circ$ . The variables examined were air temperature and specific humidity.

### 2.3. MSE calculation

MSE can be calculated as  $MSE = C_p T + gz + L_v q$  (Yanai et al., 1973), where  $C_p$  is the specific heat capacity of dry air at constant pressure (1004.6 J/kg/K);  $T$  indicates the air temperature;  $g$  is the acceleration due to gravity, with a value of 9.8 m/s;  $z$  indicates the geopotential height;  $L_v$  indicates the latent heat of vaporization of water, that is,  $2.5 \times 10^6$  J/kg; and  $q$  represents the specific humidity of the atmosphere. The examination did not consider the kinetic energy due to its negligible (thousandth) magnitude in comparison to MSE. We also examined dry static energy ( $DSE = C_p T + gz$ ) and compared the trends of MSE with those of DSE. This facilitates a better assessment of the effect of moistening in the Arctic region.

### 2.4. Moisture budget equation

To investigate the factors influencing the trend changes in Arctic moisture humidity, we conducted a moisture budget analysis. We broke down the moisture budget equation into atmospheric moisture transport

by the stationary waves (1st right-hand term), local moisture source (2nd right-hand term), and a residual term ( $\delta$ ).  $\delta$  includes the contributions from moisture transport by the transient eddies and the error from the finite difference (Seager et al., 2010; Cai et al., 2024). This aimed to enhance our understanding of the causes of moistening in the Arctic region. The formula is as follows:

$$\frac{\partial_t \langle q \rangle}{\partial t} = -\langle \nabla \cdot (\vec{V} q) \rangle + (E - P) + \delta \quad (1)$$

where operator  $\langle \rangle$  indicates density-weighted vertical integration from the surface to 300 hPa. All the variables in Eq. (1) are monthly means.

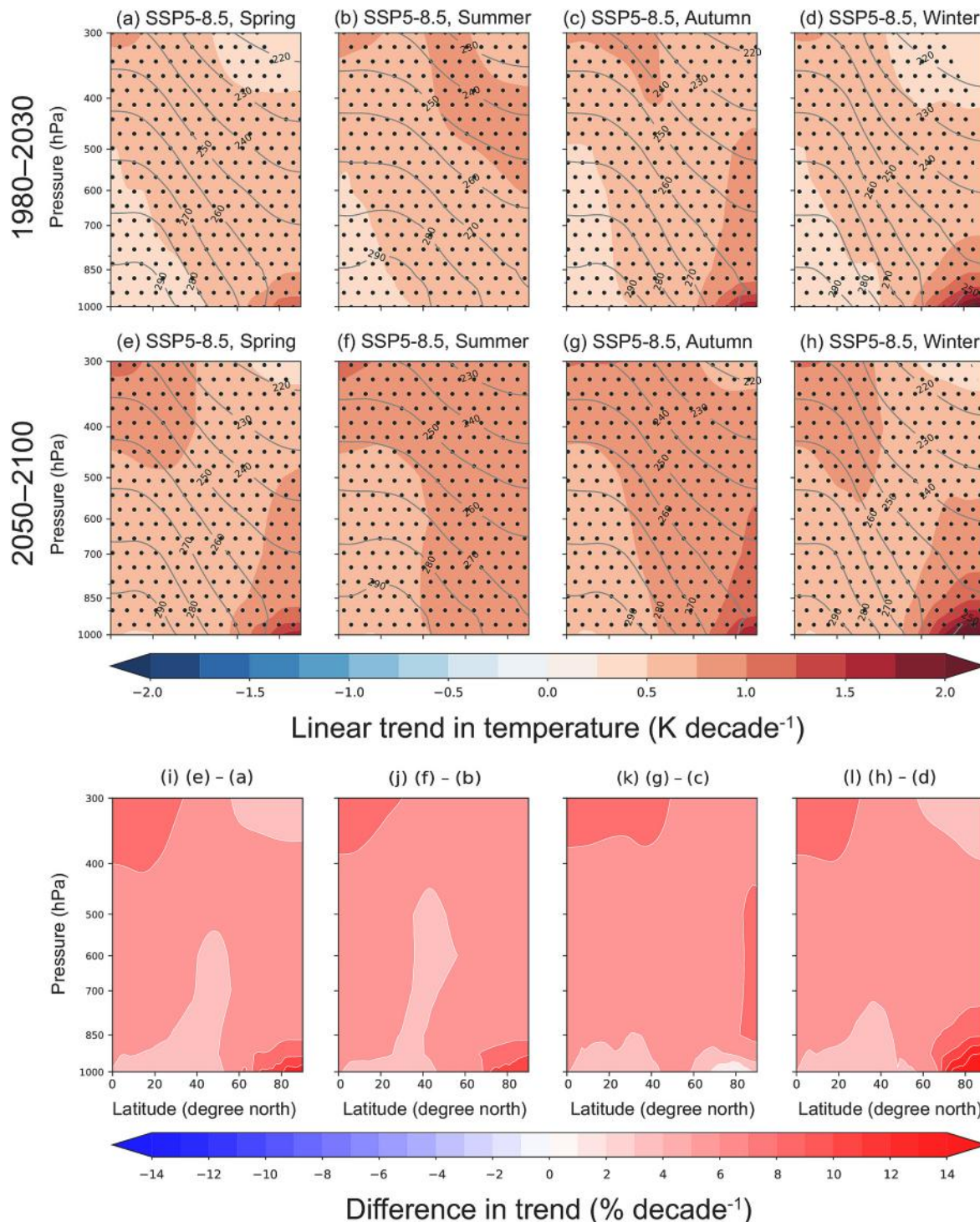


**Fig. 1.** Zonal mean 1980–2030 linear temperature trend for boreal (a) spring (March to May), (b) summer (June to August), (c) autumn (September to November), and (d) winter (December to February) based on the multi-model ensemble mean of CMIP6 historical and SSP5–8.5 experiments. The grey contours represent the climatological average temperature for 1980–2010. The dots indicate the statistical significance of the linear trends at the 95% confidence level. (e–h) Same as (a–d) but for 2050–2100. (i–l) Differences using (e–h) minus (a–d).

## 2.5. Statistical methods

The linear trend of the time series was calculated using linear regression based on the least-squares method. The statistical significance (95% confidence level,  $P < 0.05$ ) was estimated using a two-tailed Student's  $t$ -test.

## 3. Results

### 3.1. Temperature trend

Compared with the current warming (Fig. 1a–d), the future Arctic warming under the high-emission scenario is projected to accelerate (Fig. 1e–h). However, the magnitudes of Arctic warming in the current and future periods are consistently large at the bottom and sharply decreased with height, representing a bottom-heavy structure. Regardless of emission scenarios, future Arctic warming at the near-surface is

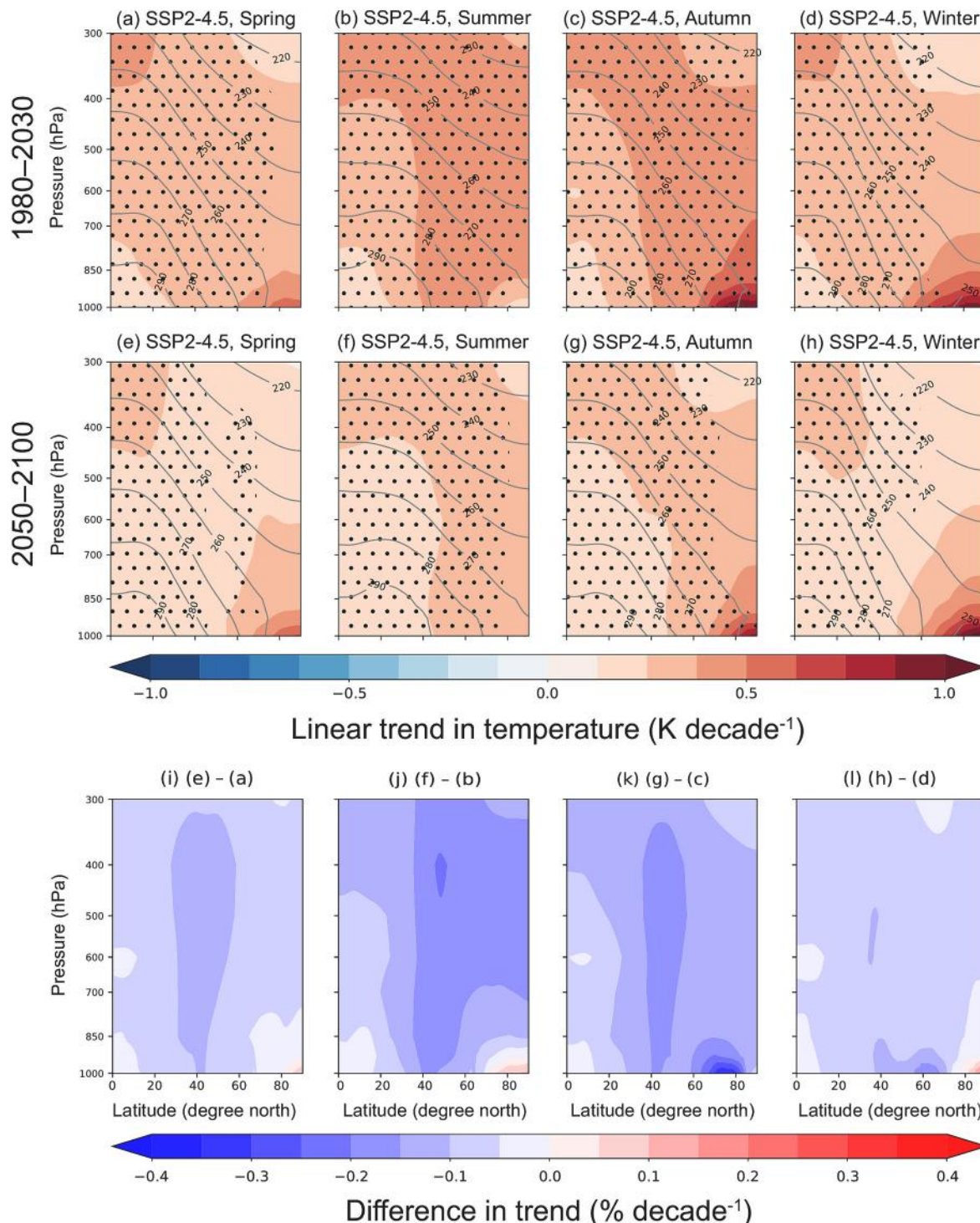


Fig. 2. Same as Fig. 1 but for SSP2-4.5.

expected to accelerate (Figs. 1 and 2). In terms of seasonality, amplified Arctic warming is observed in all seasons except for summer (Gulev et al., 2021), which is also revealed by the ERA5 reanalysis data (Fig. S2a–d). The importance of sea ice effective surface heat capacity and its accompanying local energy feedback processes in influencing the seasonality of Arctic warming is proposed to be significant (Dai et al., 2019; Boeke and Taylor, 2018; Hahn et al., 2022). Compared with warming in the current period, future accelerated warming is prominent in all seasons except for autumn (Fig. 1i–l). It is suggested that the lack of accelerated warming in autumn is related to sea ice retreat and a delay in freezing time under global warming (Xie et al., 2022a). The sea ice retreat in autumn in the future is indeed much weaker than the current, while other seasons show accelerated sea ice retreat in the future (Fig. S1). Given that future accelerated Arctic warming is also trapped at the bottom (Fig. 1i–l), the bottom-heavy vertical structure of Arctic warming is projected to remain unchanged in the future under the high-emission scenario.

When comparing future warming to the current period, a deceleration in the warming rate is projected for most of the Northern Hemisphere under the intermediate-emission scenario (Fig. 2). In contrast, the Arctic demonstrates a distinctive warming pattern, with projected bottom-heavy warming in the future surpassing the current period

(Fig. 2i–l). Notably, this accelerated warming trend is only observed in the Arctic region (Fig. 2e–h), which contrasts sharply with the pronounced magnitude changes in warming across the entire region under the high-emission scenario (Fig. 1e–h). Regarding the vertical structure, accelerated warming exhibits a prominent magnitude in the lower layers and decreases with increasing altitude, indicating an enhanced bottom-heavy structure. Decelerated warming is more pronounced in the mid-latitudes across various altitude levels (Fig. 2i–l). Additionally, in terms of seasonality, the magnitude of future warming is also weaker in autumn under the intermediate-emission scenario, particularly in the lower altitude range of 60°N to 80°N (Fig. 2k).

Both the high-emission and intermediate-emission scenarios exhibit significant uncertainty (Fig. 3). For summer, in the high-emission scenario, 21 models project a faster future warming trend, accounting for 67.7% of the total models (Fig. 3a). In contrast, in the intermediate-emission scenario, only 10 models project a faster future warming trend than the current period, accounting for 32.3% of the total models (Fig. 3c). In winter, in the high-emission scenario, 22 models project a faster future warming trend, accounting for 71.0% of the total models (Fig. 3b). In contrast, in the intermediate-emission scenario, 13 models indicate a faster future warming trend, representing 41.9% of the total models (Fig. 3d). Despite the presence of negative differences in average

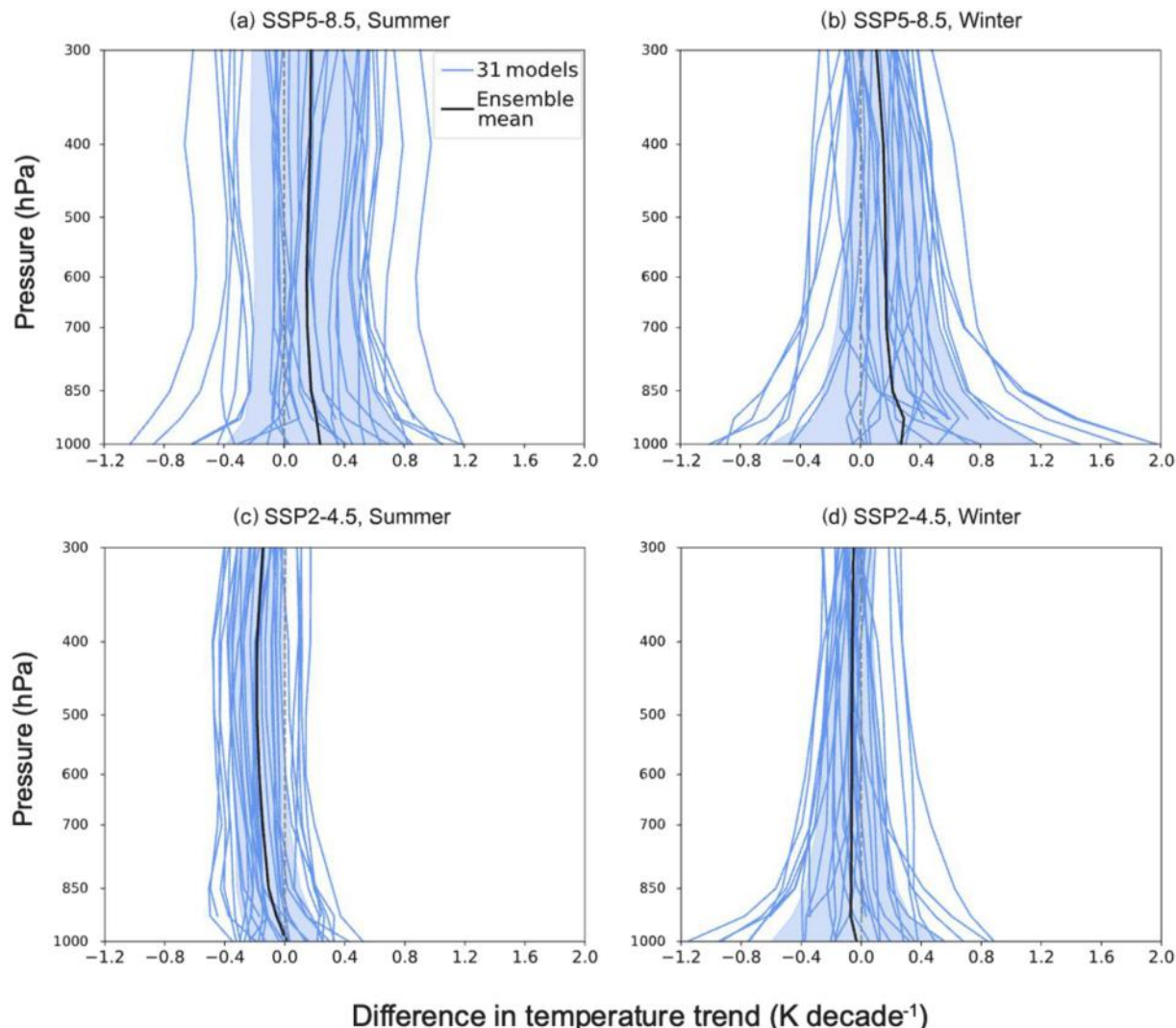


**Fig. 3.** Differences between future and current temperature trends averaged over 65°N poleward using the trend for 2050–2100 minus that for 1980–2030 during boreal (a) summer and (b) winter from the SSP5–8.5 experiment. The blue lines indicate results from individual models, and the black line indicates the multi-model ensemble mean. The blue shading indicates one standard deviation of the multi-model results. (c), (d) Same as (a), (b) but for the SSP2–4.5. (For interpretation of the references to colour in this figure legend, the reader is referred to the web version of this article.)

temperature trends at different altitudes in the intermediate-emission scenario, approximately 40% of the models project a faster future warming rate, indicating non-universal trends in Arctic temperatures under this scenario. Conversely, in the high-emission scenario, a majority of the models (around 70%) project a more substantial future Arctic warming acceleration (Fig. 3a, b). As a result, the intermediate-emission scenario shows higher levels of uncertainty compared to the high-emission scenario. Consequently, the winter projection in the high-

emission scenario is considered more reliable (Fig. 3b).

### 3.2. Humidity trend

The increasing trend of specific humidity in the tropical region is significantly higher than in the Arctic during the current period, both in the intermediate-emission and high-emission scenarios (Fig. 4a-d). The rate of specific humidity growth is notably higher in summer compared

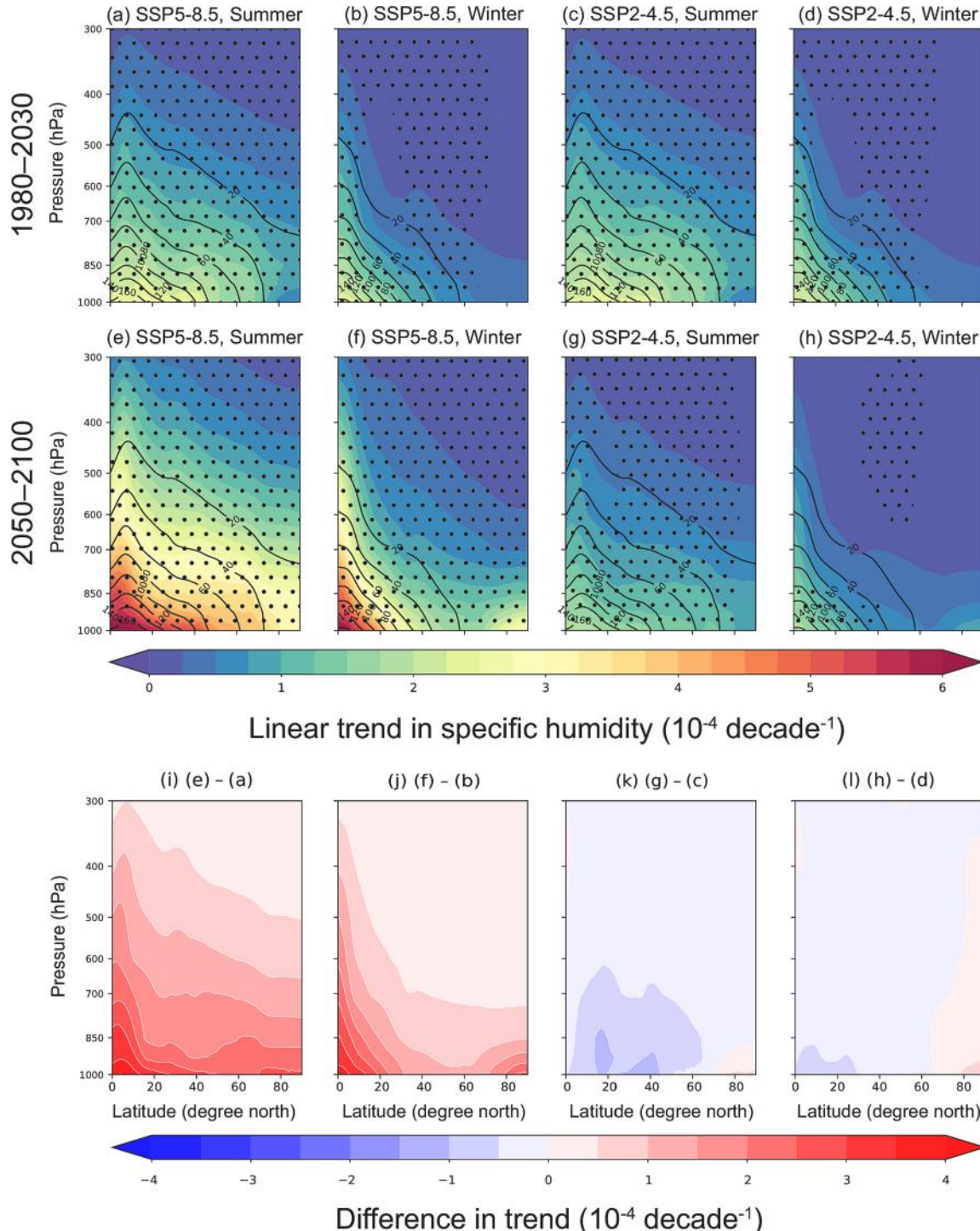


**Fig. 4.** Zonal mean 1980–2030 linear trend in specific humidity for boreal (a) summer, (b) winter based on the multi-model ensemble mean of CMIP6 historical and SSP5–8.5 experiments. (c, d) Same as (a, b) but for SSP2–4.5. The black contours represent the climatological average specific humidity for 1980–2010. The dots indicate the statistical significance of the linear trends at the 95% confidence level. (e–h) Same as (a–d) but for 2050–2100. (i–l) Differences using (e–h) minus (a–d). Results for spring and autumn are presented in Fig. S5.

to winter (Fig. 4a–d). However, despite the accelerated moistening trend observed in the tropical region, there will be a significant increase in specific humidity in the Arctic during the winter in the future (Fig. 4f, h). Due to the weaker convection in the Arctic compared to the tropics, the acceleration in humidity in the Arctic will be more concentrated in the lower layers, indicating a strong bottom-heavy structure similar to warming. Comparing with the current period (Fig. 4a–d) and taking into account the changes seen in the intermediate-emission scenario and high-emission scenario (Fig. 4i–l), it is evident that the vertical structure of future Arctic moistening is projected to remain unchanged,

maintaining a bottom-heavy structure (Fig. 4e–h). Note that the ERA5 reanalysis data also show the bottom-heavy structure (Fig. S2e–h). However, the enhanced increase in specific humidity in the tropical region relative to the Arctic is not as strong as that in CMIP6 simulations; that is, the specific humidity increase in the Arctic relative to lower latitudes is more evident in ERA5 reanalysis than in CMIP6 simulations.

Climatological water vapor distribution varies significantly with latitude. To address this non-uniformity, we conducted a further analysis by normalizing the specific humidity values at each latitude with the climatological mean specific humidity at 1000–850 hPa from 1980 to

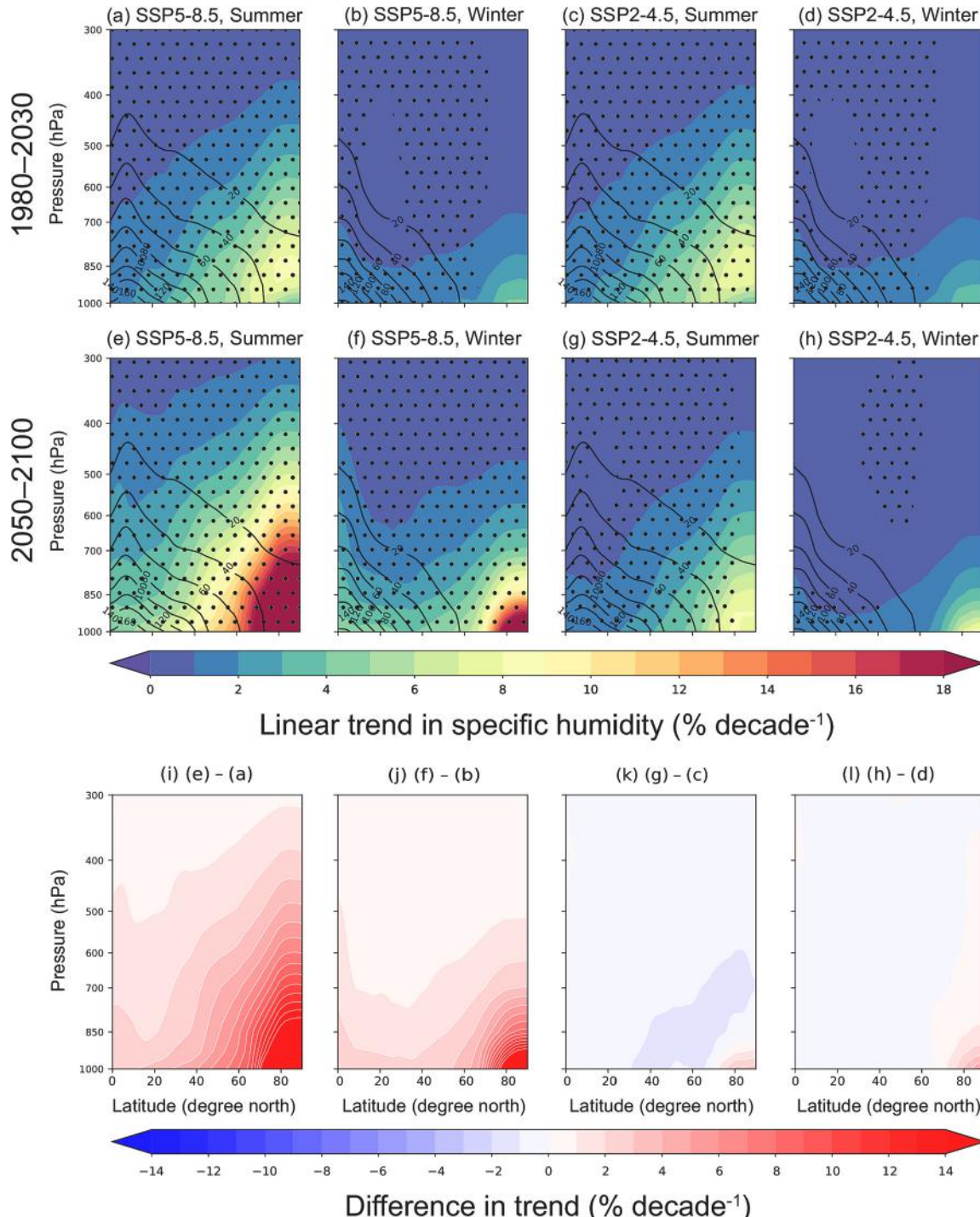


**Fig. 5.** Same as Fig. 4 but for the percentage change in specific humidity, which was calculated as the specific humidity trend divided by the 1000–850 hPa climatological mean specific humidity for 1980–2014. Results for spring and autumn are presented in Fig. S6.

2014. This allowed us to examine the percentage changes in humidity. During the current period, specific humidity is significantly increased compared to the climatological mean, with a sharp increase from the tropical to the Arctic, namely, an Arctic moistening amplification (Fig. 5a–d). In terms of seasonality, the acceleration in moistening is particularly pronounced in the Arctic during the summer. In the high-emission scenario, there is a distinct bottom-heavy structure in the specific humidity acceleration, with localized enhancements exceeding 18% in the mid-to-high latitudes (Fig. 5e). Although the magnitude of specific humidity increase is lower in the future under the intermediate-emission scenario compared to the high-emission scenario (Fig. 5e–h), the vertical structure of Arctic moistening amplification remains similar between the two scenarios.

The projections of specific humidity increase are more reliable under the high-emission scenario (Fig. 6a, b). Specifically, relative to current change, 30 models project a faster future increase in specific humidity at the lower atmosphere during the summer, and all models project a faster increase during the winter. The increase in specific humidity is more pronounced during the summer, approximately 1.5 times higher than during the winter (Fig. 6a, b). In contrast, there are significant discrepancies in specific humidity changes among the 31 models under the intermediate-emission scenario (Fig. 6c, d). During the summer, 14 models project a faster increase in specific humidity at the lower atmosphere in the future compared to the current period, accounting for

45.2% of the total models, which is almost equivalent to the number of models projecting a deceleration in specific humidity increase (Fig. 6c). Therefore, it can be concluded that under the high-emission scenario, future specific humidity will increase more rapidly than the current period, exhibiting a bottom-heavy structure.

### 3.3. MSE trend

MSE combines temperature and humidity and is a crucial variable for understanding the thermodynamic and dynamic characteristics of the moist atmosphere (Yanai et al., 1973; Graversen and Burtu, 2016; Hill et al., 2017). MSE can also explicitly depict the effect of latent heat change on the temperature of the moist atmosphere, similar to equivalent temperature and equivalent potential temperature (Matthews et al., 2022; Song et al., 2022). Therefore, it is essential to utilize MSE to examine the combined effects of Arctic warming and moistening. Based on MSE, the “Arctic amplification” is pronounced in winter but not significant in summer during the current period (Fig. 7a–d). In the future, under the intermediate-emission scenario, MSE is projected to increase at a slower rate in the Northern Hemisphere, while the Arctic region experiences accelerated changes (Fig. 7e, f). Under the high-emission scenario, the MSE-based Arctic amplification is expected to intensify in both summer and winter (Fig. 7g, h). Similar to temperature and humidity (Figs. 1, 2, 4), the current and future periods exhibit a

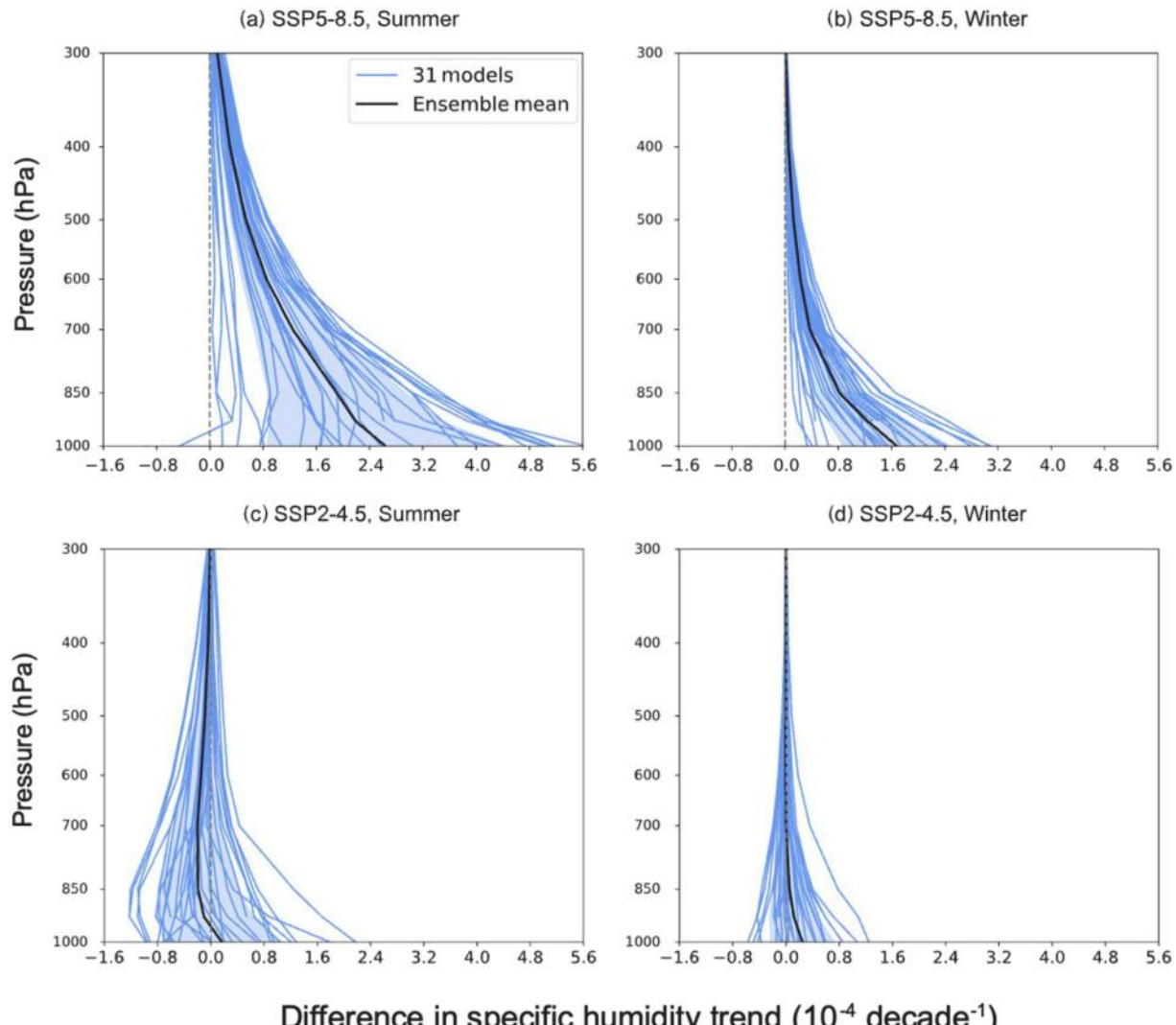


Fig. 6. Same as Fig. 3 but for specific humidity.

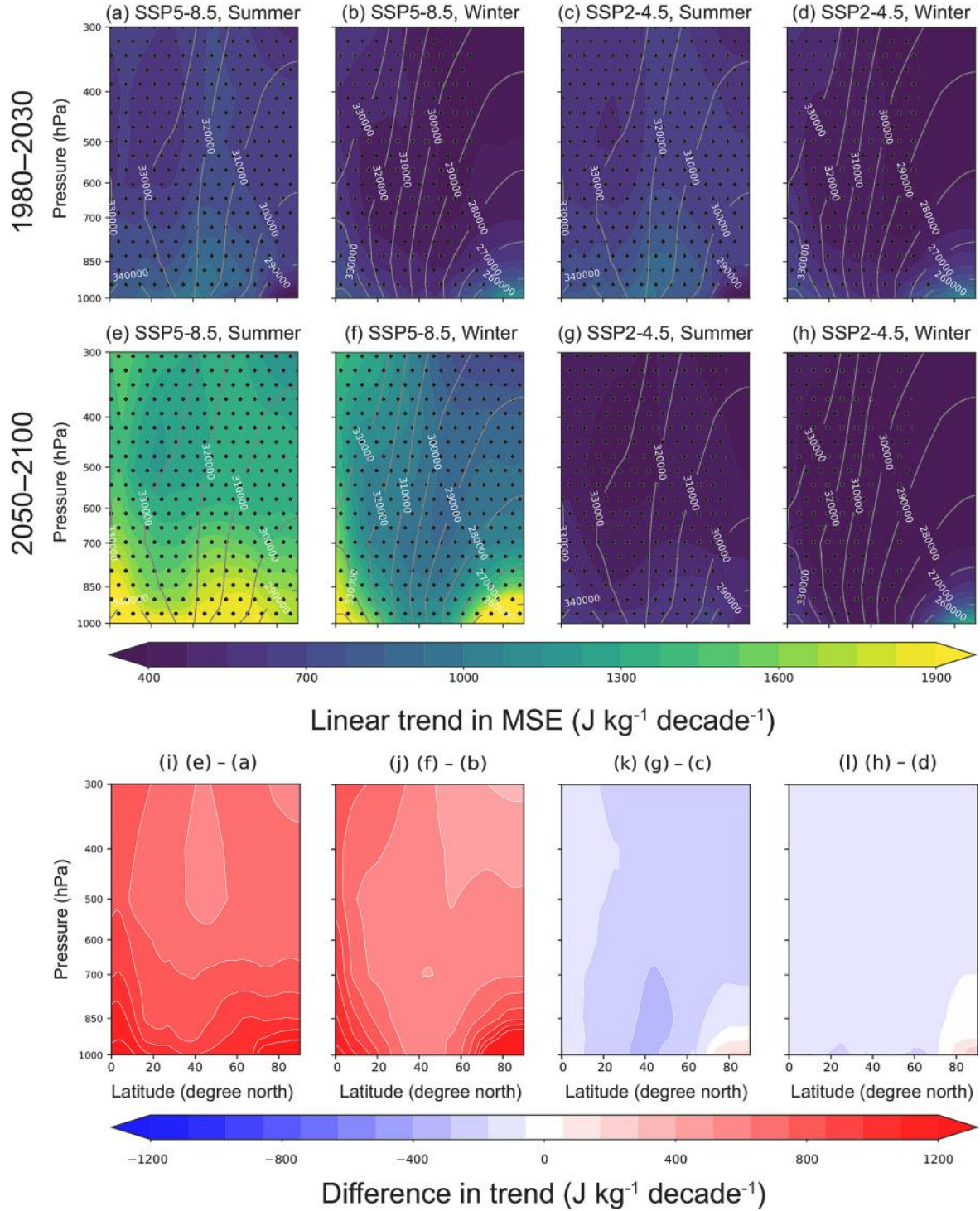


Fig. 7. Same as Fig. 4 but for moist static energy (MSE). Results for spring and autumn are presented in Fig. S7.

bottom-heavy structure in the growth of MSE (Fig. 7). The future strengthening of the MSE-based Arctic amplification, compared to the current period, will be determined by the combined influences of warming (DSE change) and moistening (latent heat change) under the high-emission scenario. Although the contribution of DSE change to the MSE change is higher than that of latent heat change (Figs. S3 and S4), the contribution of latent heat change is not negligible. For example, the magnitude of near-surface latent heat change in the Arctic is almost half of the MSE change in summer (Figs. S3j and S4j). Due to the lack of accelerated changes in temperature and humidity under the

intermediate-emission scenario, the acceleration of MSE growth is lacking.

The results regarding future MSE change under the high-emission scenario are also more reliable than those for the intermediate-emission scenario (Fig. 8). 28 models project an accelerated increase in Arctic MSE during summer, and 29 models project an accelerated increase during winter under the high-emission scenario, which represents over 90% of the total models (Fig. 8a, b). In contrast, there are significant differences in Arctic MSE changes among the 31 models under the intermediate-emission scenario (Fig. 8c, d). For instance,

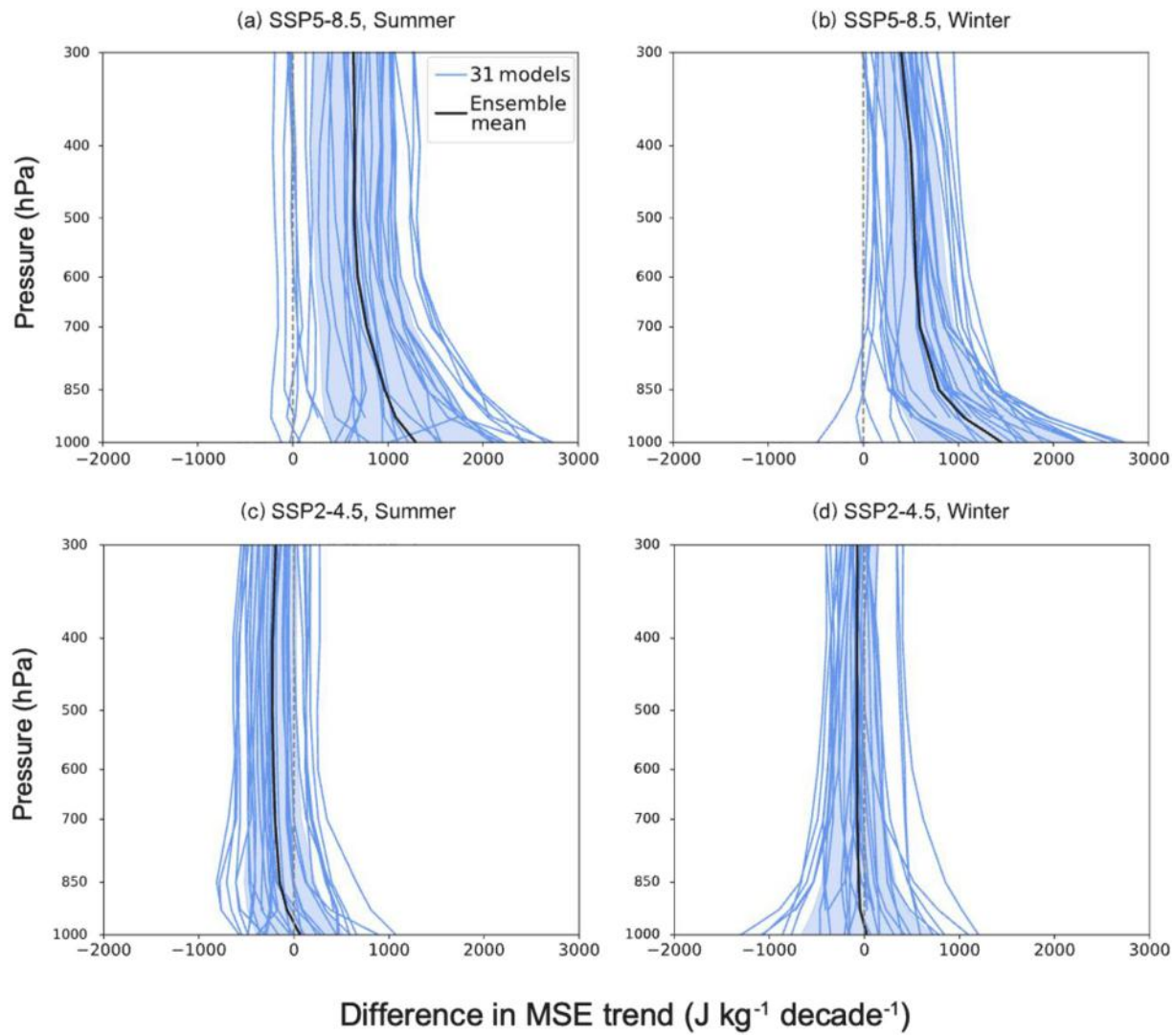


Fig. 8. Same as Fig. 3 but for MSE.

during winter under the intermediate-emission scenario, 15 models project an accelerated increase in future Arctic MSE, accounting for 48.4% of the total models (Fig. 8d), and the average line hovers around the zero baseline. Therefore, it can be concluded that under the high-emission scenario in the future, the growth of Arctic MSE will accelerate.

#### 3.4. Mechanisms for humidity changes

Relative to studies on Arctic warming mechanisms, research on humidity remains insufficient. Therefore, we further explored the processes contributing to the increase in humidity. For the Arctic region, two factors influencing atmospheric humidity are meridional atmospheric moisture transport from lower latitudes and the local moisture source ( $E - P$ ) (Vihma et al., 2016; Bintanja et al., 2020; Cai et al., 2024). In the calculation utilizing the moisture budget equation (Eq. (1)), the meridional atmospheric moisture transport is partitioned into two components: the first component represents the transport by the stationary waves, as indicated by the first term on the right-hand side; the second component represents the transport by the transient eddies, which is encompassed in the third term on the right-hand side. The local moisture source is represented by evaporation minus precipitation ( $E - P$ ).

In the current period, negative trends in  $E - P$  are observed in the Arctic region (Fig. 9). Consequently, the observed increase in Arctic

humidity cannot be attributed to a strengthening of local moisture source. In the future, both the intermediate-emission and high-emission scenarios project negative  $E - P$  trends in the Arctic region during the summer (Fig. 9a, c). However, under the high-emission scenario, the  $E - P$  trend in the Arctic region becomes positive during the winter. In both scenarios, except for winter in the future under the intermediate-emission scenario, the trends in the Arctic region during the current and future periods pass the significance test, enabling reliable conclusions to be drawn. Future accelerated Arctic moistening cannot be driven by the local moisture source, except for an enhanced local moisture source during winter under the high-emission scenario (Fig. 9b). This implies that enhanced meridional atmospheric moisture transport should be responsible for the Arctic moistening except for winter under the high-emission scenario. The subsequent demonstration will showcase the respective roles of stationary waves and transient eddies in meridional atmospheric moisture transport.

In addition to local moisture sources (Fig. 9), the water vapor supplies to the Arctic induced by meridional atmospheric moisture transport due to stationary waves and transient eddies are shown in Figs. 10 and 11, respectively. In the current period for both high- and intermediate-emission scenarios, moisture transport by transient eddies dominated Arctic moistening during the summer, and moisture transport by stationary waves further increased the moistening about 80°N poleward (Figs. 10a,c and 11a,c). The accelerated Arctic moistening in

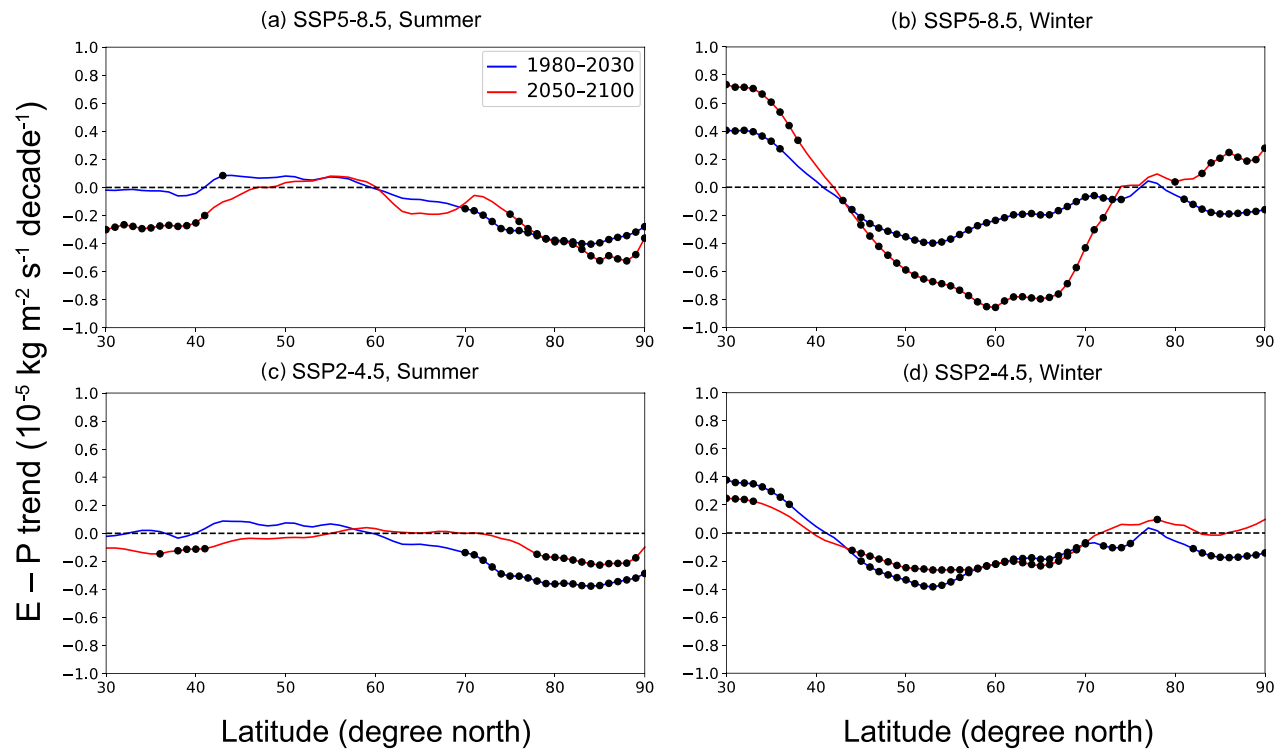


**Fig. 9.** Zonal mean 2050–2100 (red) and 1980–2030 (blue) linear trends in evaporation minus precipitation ( $E - P$ ) during boreal (a) summer and (b) winter for SSP5-8.5. The dots indicate the statistical significance of the linear trends at the 95% confidence level. (c), (d) Same as (a), (b) but for the SSP2-4.5. (For interpretation of the references to colour in this figure legend, the reader is referred to the web version of this article.)

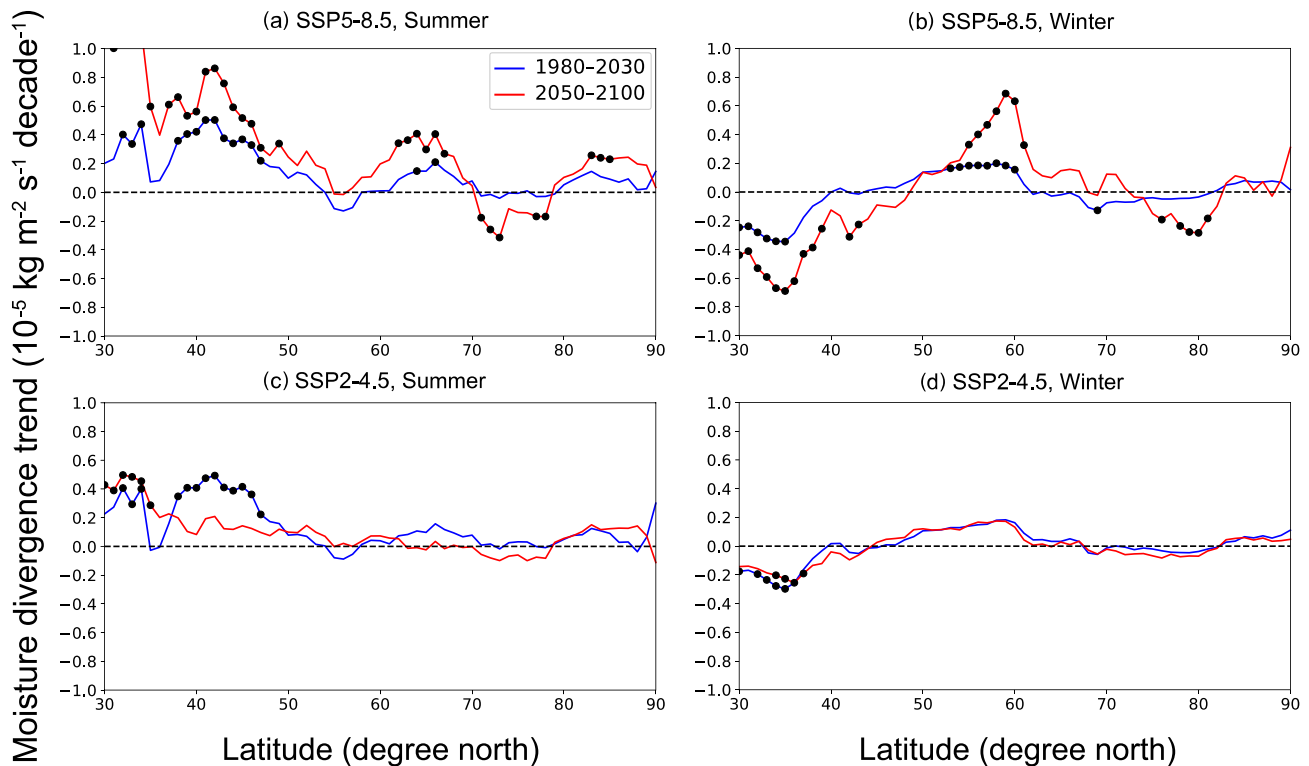


**Fig. 10.** Same as Fig. 9 but for moisture divergence induced by the stationary wave transport (1st right-hand term of Eq. (1)), in which positive and negative values mean moisture convergence and divergence, respectively.

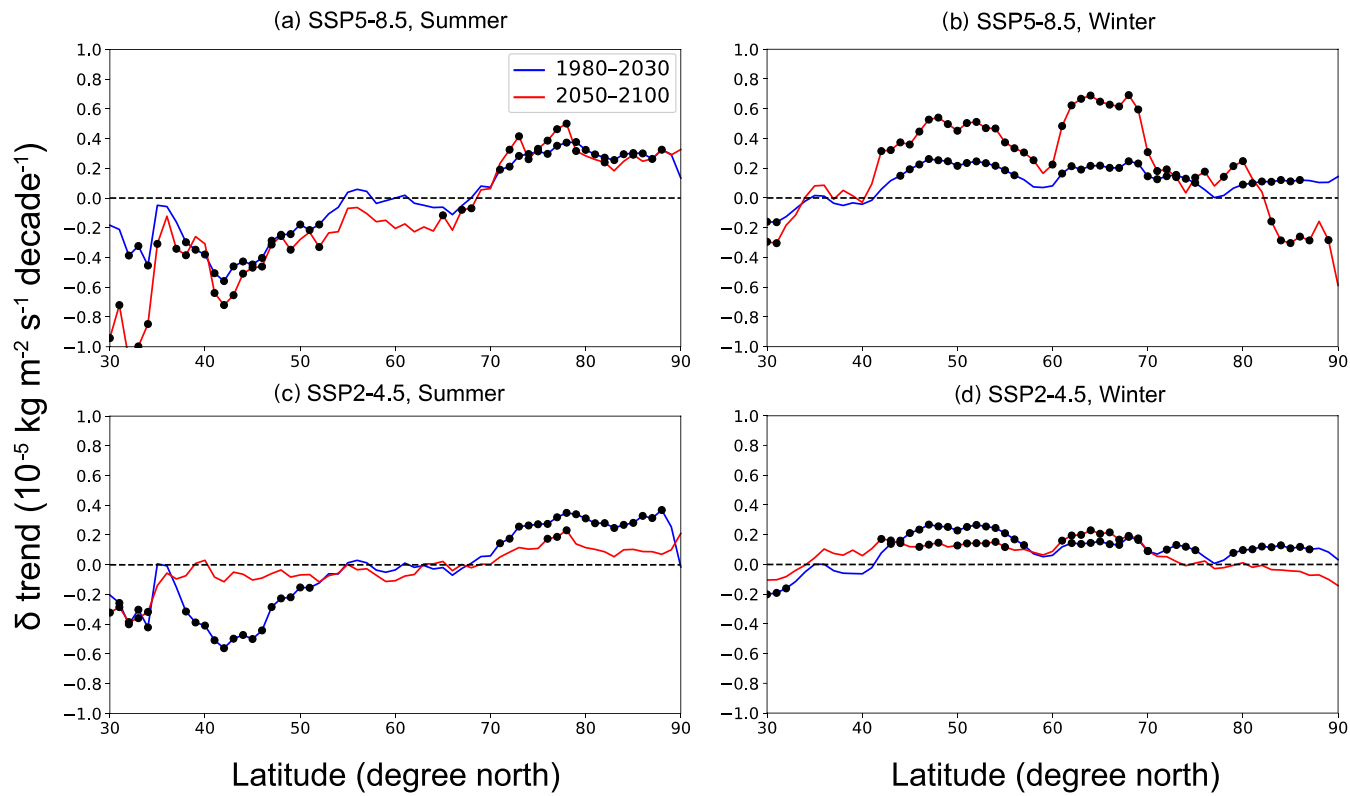


**Fig. 11.** Same as [Fig. 10](#) but for the residual term  $\delta$  in Eq. (1), which includes the moisture divergence induced by the transient eddy transport.

the future under the high-emission scenario is determined by the enhanced stationary wave-transported moisture towards the North Pole during the summer ([Fig. 10a](#)). In addition, the much weaker transient eddy-transported moisture in the future than the current hinders the future accelerated Arctic moistening during the summer under the intermediate-emission scenario ([Fig. 11c](#)).

During the winter, under the high-emission scenario, the trends in stationary wave-transported moisture are almost negative in the Arctic ([Fig. 10b](#)). The trends in transient eddy-transported moisture are positive south 80°N but negative poleward in the future ([Fig. 11b](#)). The negative moisture transport into the Arctic suppresses its moistening. Therefore, the accelerated Arctic moistening in the future under the high-emission scenario is due to the enhanced local moisture source during winter ([Fig. 9b](#)). For the intermediate-emission scenario, the situation in the winter is similar to that in the summer.

In the high-emission scenario, 74.2% of the models project a negative future-minus-current difference in the  $E - P$  trend during the summer in the Arctic region, while 71.0% project a positive difference in the  $E - P$  trend during the winter ([Fig. 12a, b](#)). In contrast, the projections under the intermediate-emission scenario exhibit higher uncertainty ([Fig. 12c, d](#)). For the intermediate-emission scenario, 19 models project a positive future-minus-current difference in the  $E - P$  trend during summer in the Arctic region, accounting for 61.3% of the total models ([Fig. 12c](#)). Meanwhile, 11 models project a positive future-minus-current difference in the  $E - P$  trend during winter, representing 35.5% of the total models. Relative to the local moisture source, the meridional atmospheric moisture transport shows larger inter-model discrepancies ([Figs. S8 and S9](#)). Hence, it can be concluded that the projections of future changes in the hydrological cycle in the Arctic region are also more reliable under the high-emission scenario compared to the intermediate-emission scenario. Under the high-emission scenario, the increased Arctic moistening in the future is caused by the meridional atmospheric moisture transport during the summer and the local moisture supply during the winter.

#### 4. Discussion and conclusions

This study reveals that Arctic warming will accelerate in the future under high-emission scenarios. However, the bottom-heavy structure of Arctic warming is projected to remain unchanged. Additionally, under the high-emission scenario, future Arctic moistening is expected to be more pronounced than the present level. The vertical structure of Arctic moistening exhibits a similar bottom-heavy pattern as warming. Notably, there is higher uncertainty among models under the intermediate-emission scenario, indicating low reliability of the results. In contrast, the results among models under the high-emission scenario show higher consistency and credibility. The accelerated future Arctic moistening will be controlled by enhanced poleward atmospheric moisture transport during the summer and an enhanced local moisture source during the winter. The joint influence of warming and moistening will lead to an accelerated increase in MSE while maintaining the bottom-heavy structure. Therefore, the vertical structures of Arctic warming in both dry and moist (with the effect of latent heat explicitly depicted) atmospheres are projected to remain unchanged.

The response of mid-latitude atmospheric circulation to Arctic warming depends on the vertical structure of Arctic warming, as demonstrated by previous studies ([He et al., 2020](#); [Labe et al., 2020](#); [Xie et al., 2020](#); [Kim et al., 2021](#)). The findings of this study, which indicate the unchanged vertical structures of Arctic warming in both dry and moist atmospheres, suggest that the regimes of the response of mid-latitude circulation mediated by the vertical structure of Arctic warming will likely remain unchanged. However, it is important to note that this study does not consider the vertical structure of Arctic temperature or humidity anomalies at the synoptic scale ([He et al., 2020](#)). In addition, atmospheric vortices via high-frequency turbulent transport can also influence the meridional transport of MSE, leading to climate change in the Arctic region ([Graversen and Burtu, 2016](#); [Feldl et al., 2017](#)). Therefore, further investigations are needed to explore future changes in the Arctic climate on other time scales, such as synoptic

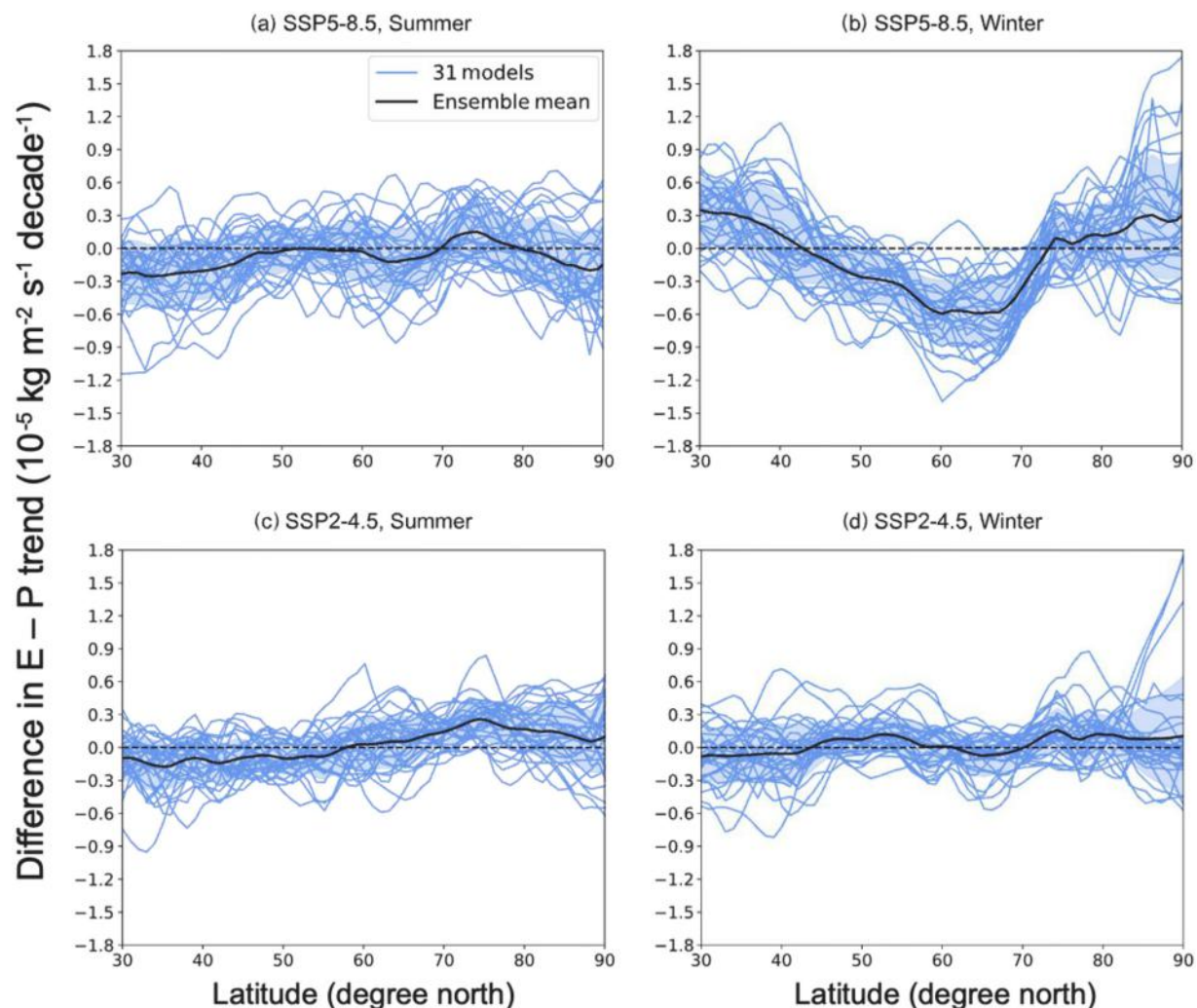


**Fig. 12.** Differences between future and current trends of  $E - P$  using the trend for 2050–2100 minus that for 1980–2030 during boreal (a) summer and (b) winter from the SSP5-8.5 experiment. The blue lines indicate results from individual models, and the black line indicates the multi-model ensemble mean. The blue shading indicates one standard deviation of the multi-model results. (c), (d) Same as (a), (b) but for the SSP2-4.5. (For interpretation of the references to colour in this figure legend, the reader is referred to the web version of this article.)

variability, under global warming.

#### CRediT authorship contribution statement

**Hanbin Nie:** Data curation, Formal analysis, Investigation, Software, Validation, Visualization, Writing – original draft, Writing – review & editing. **Yongkun Xie:** Conceptualization, Data curation, Formal analysis, Funding acquisition, Investigation, Methodology, Project administration, Supervision, Validation, Writing – original draft, Writing – review & editing. **Min Zhao:** Formal analysis, Investigation, Validation, Writing – review & editing. **Zifan Su:** Software, Visualization, Writing – review & editing.

#### Declaration of competing interest

The authors declare that they have no known competing financial interests or personal relationships that could have appeared to influence the work reported in this paper.

#### Data availability

All data are publicly available on CMIP6 official website at <https://esgf-node.llnl.gov/search/cmip6/>. ERA5 data can be accessed at

the ECMWF website <https://cds.climate.copernicus.eu/cdsapp#!/dataset/reanalysis-era5-pressure-levels-monthly-means?tab=form>.

#### Acknowledgments

We thank the anonymous reviewers for their constructive comments. We thank World Climate Research Programme's Working Group on Coupled Modelling and the institutes participating in CMIP6 for sharing their model outputs. We thank ECMWF for providing the reanalysis data. This work was supported by National Natural Science Foundation of China (42030602, 91937302), the Fundamental Research Funds for the Central Universities (Izujbky-2022-kb10), and the Gansu Provincial Special Fund Project for Guiding Scientific and Technological Innovation and Development (2019ZX-06).

#### Appendix A. Supplementary data

Supplementary data to this article can be found online at <https://doi.org/10.1016/j.atmosres.2024.107271>.

## References

Barnes, E.A., Polvani, L.M., 2015. CMIP5 projections of Arctic amplification, of the North American/North Atlantic circulation, and of their relationship. *J. Clim.* 28 (13), 5254–5271. <https://doi.org/10.1175/jcli-d-14-00589.1>.

Bintanja, R., van der Wiel, K., Van der Linden, E.C., Reusen, J., Bogerd, L., Krikken, F., Selten, F.M., 2020. Strong future increases in Arctic precipitation variability linked to poleward moisture transport. *Sci. Adv.* 6 (7), eaax6869. <https://doi.org/10.1126/sciadv.aax6869>.

Boeke, R.C., Taylor, P.C., 2018. Seasonal energy exchange in sea ice retreat regions contributes to differences in projected Arctic warming. *Nat. Commun.* 9, 5017. <https://doi.org/10.1038/s41467-018-07061-9>.

Cai, M., 2005. Dynamical amplification of polar warming. *Geophys. Res. Lett.* 32, L22710. <https://doi.org/10.1029/2005GL024481>.

Cai, Z., You, Q., Wu, F., Chen, H.W., Chen, D., Cohen, J., 2021. Arctic warming revealed by multiple CMIP6 models: evaluation of historical simulations and quantification of future projection uncertainties. *J. Clim.* 34, 4871–4892. <https://doi.org/10.1175/JCLI-D-20-0791.1>.

Cai, Z., You, Q., Chen, H., Zhang, R., Chen, D., Chen, J., Kang, S., Cohen, J., 2022. Amplified wintertime Barents Sea warming linked to intensified Barents oscillation. *Environ. Res. Lett.* 17 (4), 044068. <https://doi.org/10.1088/1748-9326/ac5bb3>.

Cai, Z., You, Q., Chen, H., Zhang, R., Zuo, Z., Chen, D., Cohen, J., Screen, J., 2024. Assessing arctic wetting: performances of CMIP6 models and projections of precipitation changes. *Atmos. Res.* 297, 107124. <https://doi.org/10.1016/j.atmosres.2023.107124>.

Cohen, J., Zhang, X., Francis, J., Jung, T., Kwok, R., Overland, J., Ballinger, T.J., Bhatt, U.S., Chen, H.W., Coumou, D., Feldstein, S., Gu, H., Handorf, D., Henderson, G., Ionita, M., Kretschmer, M., Laliberte, F., Lee, S., Linderholm, H.W., Yoon, J., 2019. Divergent consensuses on Arctic amplification influence on midlatitude severe winter weather. *Nat. Clim. Chang.* 10 (1), 20–29. <https://doi.org/10.1038/s41558-019-00622-y>.

Dai, A., Luo, D., Song, M., Liu, J., 2019. Arctic amplification is caused by sea-ice loss under increasing CO<sub>2</sub>. *Nat. Commun.* 10 (1), 121. <https://doi.org/10.1038/s41467-018-07954-9>.

Delworth, T.L., Zeng, F., Vecchi, G.A., Yang, X., Zhang, L., Zhang, R., 2016. The North Atlantic Oscillation as a driver of rapid climate change in the Northern Hemisphere. *Nat. Geosci.* 9 (7), 509–512. <https://doi.org/10.1038/ngeo2738>.

Deser, C., Tomas, R., Alexander, M., Lawrence, D., 2010. The seasonal atmospheric response to projected Arctic Sea ice loss in the late twenty-first century. *J. Clim.* 23, 333–351. <https://doi.org/10.1175/2009JCLI3053.1>.

Ding, S., Wu, B., Chen, W., 2021. Dominant characteristics of early Autumn Arctic sea ice variability and its impact on Winter Eurasian climate. *J. Clim.* 34, 1825–1846. <https://doi.org/10.1175/JCLI-D-19-0834.1>.

Docquier, D., Koenigk, T., 2021. Observation-based selection of climate models projects Arctic ice-free summers around 2035. *Commun. Earth Environ.* 2, 144. <https://doi.org/10.1038/s43247-021-00214-7>.

Duan, A., Peng, Y., Liu, J., Chen, Y., Wu, G., Holland, D.M., et al., 2022. Sea ice loss of the Barents-Kara Sea enhances the winter warming over the Tibetan Plateau. *npj Clim. Atmos. Sci.* 5 (1), 26. <https://doi.org/10.1038/s41612-022-00245-7>.

Eyring, V., Bony, S., Meehl, G.A., Senior, C.A., Stevens, B., Stouffer, R.J., Taylor, K.E., 2016. Overview of the Coupled Model Intercomparison Project Phase 6 (CMIP6) experimental design and organization. *Geosci. Model Dev.* 9 (5), 1937–1958. <https://doi.org/10.5194/gmd-9-1937-2016>.

Feldl, N., Anderson, B., Bordonali, S., 2017. Atmospheric eddies mediate lapse rate feedback and Arctic amplification. *J. Clim.* 30, 9213–9224. <https://doi.org/10.1175/JCLI-D-16-0706.1>.

Francis, J.A., Vavrus, S.J., 2012. Evidence linking Arctic amplification to extreme weather in mid-latitudes. *Geophys. Res. Lett.* 39 (6), L06801. <https://doi.org/10.1029/2012gl051000>.

Gao, K., Duan, A., Chen, D., Wu, G., 2019. Surface energy budget diagnosis reveals possible mechanism for the different warming rate among the three poles on Earth in recent decades. *Sci. Bull.* 64 (16), 1140–1143. <https://doi.org/10.1016/j.scib.2019.06.023>.

Graversen, R.G., Burtu, M., 2016. Arctic amplification enhanced by latent energy transport of atmospheric planetary waves. *Q. J. R. Meteorol. Soc.* 142, 2046–2054. <https://doi.org/10.1002/qj.2802>.

Graversen, R.G., Mauritsen, T., Tjernstrom, M., Kallen, E., Svensson, G., 2008. Vertical structure of recent Arctic warming. *Nature* 451 (7174), 53–56. <https://doi.org/10.1038/nature06502>.

Gulev, S.K., Thorne, P.W., Ahn, J., Dentener, F.J., Domingues, C.M., Gerland, S., Vose, R.S., 2021. Changing state of the climate system. In: *In Climate Change 2021: The Physical Science Basis. Contribution of Working Group I to the Sixth Assessment Report of the Intergovernmental Panel on Climate Change*. Cambridge University Press.

Hahn, L.C., Armour, K.C., Battisti, D.S., Eisenman, I., Bitz, C.M., 2022. Seasonality in Arctic warming driven by sea ice effective heat capacity. *J. Clim.* 35, 1629–1642. <https://doi.org/10.1175/JCLI-D-21-0626.1>.

He, S., Xu, X., Furevik, T., Gao, Y., 2020. Eurasian cooling linked to the vertical distribution of Arctic warming. *Geophys. Res. Lett.* 47 (10) <https://doi.org/10.1029/2020gl087212> e2020GL087212.

Held, I.M., Soden, B.J., 2006. Robust responses of the hydrological cycle to global warming. *J. Clim.* 19, 5686–5699.

Hersbach, H., Bell, B., Berrisford, P., et al., 2020. The ERA5 global reanalysis. *Q. J. R. Meteorol. Soc.* 146, 1999–2049. <https://doi.org/10.1002/qj.3803>.

Hill, S.A., Ming, Y., Held, I.M., Zhao, M., 2017. A moist static energy budget-based analysis of the Sahel rainfall response to uniform oceanic warming. *J. Clim.* 30, 5637–5660. <https://doi.org/10.1175/jcli-d-16-0785.1>.

Hoskins, B.J., McIntyre, M., Robertson, A.W., 1985. On the use and significance of isentropic potential vorticity maps. *Q. J. R. Meteorol. Soc.* 111 (470), 877–946. <https://doi.org/10.1002/qj.49711147002>.

Huang, J., Zhang, X., Zhang, Q., Lin, Y., Hao, M., Luo, Y., Zhao, Z., Yao, Y., Chen, X., Wang, L., Nie, S., Yin, Y., Xu, Y., Zhang, J., 2017. Recently amplified arctic warming has contributed to a continual global warming trend. *Nat. Clim. Chang.* 7 (12), 875–879. <https://doi.org/10.1038/s41558-017-0009-5>.

Kim, K.-Y., Kim, J.-Y., Kim, J., Yeo, S., Na, H., Hamlington, B.D., Leben, R.R., 2019. Vertical feedback mechanism of winter Arctic amplification and sea ice loss. *Sci. Rep.* 9, 1184. <https://doi.org/10.1038/s41598-018-38109-x>.

Kim, D., Kang, S.M., Merlis, T.M., Shin, Y., 2021. Atmospheric circulation sensitivity to changes in the vertical structure of polar warming. *Geophys. Res. Lett.* 48 (19) <https://doi.org/10.1029/2021gl094726> e2021GL094726.

Labe, Z., Peings, Y., Magnusdottir, G., 2020. Warm Arctic, cold Siberia pattern: role of full Arctic amplification versus sea ice loss alone. *Geophys. Res. Lett.* 47 (17) <https://doi.org/10.1029/2020gl088583> e2020GL088583.

Li, J., Wu, Z., 2012. Importance of autumn Arctic sea ice to northern winter snowfall. *Proc. Natl. Acad. Sci. USA* 109 (28), 1898. <https://doi.org/10.1073/pnas.1205075109>.

Lu, J., Cai, M., 2009. Seasonality of polar surface warming amplification in climate simulations. *Geophys. Res. Lett.* 36, L16704. <https://doi.org/10.1029/2009GL040133>.

Luo, D., Chen, X., Overland, J., Simmonds, I., Wu, Y., Zhang, P., 2019. Weakened potential vorticity barrier linked to recent winter Arctic Sea ice loss and midlatitude cold extremes. *J. Clim.* 32 (14), 4235–4261. <https://doi.org/10.1175/JCLI-D-18-0449.1>.

Luo, B., Luo, D., Ge, Y., Dai, A., Wang, L., Simmonds, I., Xiao, C., Wu, L., Yao, Y., 2023. Origins of Barents-Kara sea-ice interannual variability modulated by the Atlantic pathway of El Niño-Southern Oscillation. *Nat. Commun.* 14 (1), 585. <https://doi.org/10.1038/s41467-023-36136-5>.

Matthews, T., Byrne, M., Horton, R., Murphy, C., Pielke, R., Raymond, C., Thorne, P., Wilby, R.L., 2022. Latent heat must be visible in climate communications. *WIREs Clim. Chang.* 13 (4), e779. <https://doi.org/10.1002/wcc.779>.

Nakamura, T., Yamazaki, K., Iwamoto, K., Honda, M., Miyoshi, Y., Ogawa, Y., Ukita, J., 2015. A negative phase shift of the winter AO/NAO due to the recent Arctic sea-ice reduction in late autumn. *J. Geophys. Res. Atmos.* 120 (8), 3209–3227. <https://doi.org/10.1002/2014jd022848>.

Notz, D., Stroeve, J., 2018. The trajectory towards a seasonally ice-free Arctic Ocean. *Curr. Clim. Chang. Rep.* 4 (4), 407–416. <https://doi.org/10.1007/s40641-018-0113-2>.

O'Neill, B.C., Kriegler, E., Ebi, K.L., Kemp-Benedict, E., Riahi, K., Rothman, D.S., van Ruijven, B.J., van Vuuren, D.P., Birkmann, J., Kok, K., Levy, M., Solecki, W., 2017. The roads ahead: Narratives for shared socioeconomic pathways describing world futures in the 21st century. *Glob. Environ. Chang.* 42, 169–180. <https://doi.org/10.1016/j.gloenvcha.2015.01.004>.

Overland, J.E., Wang, M., 2013. When will the summer Arctic be nearly sea ice free? *Geophys. Res. Lett.* 40 (10), 2097–2101. <https://doi.org/10.1002/grl.50316>.

Papritz, L., 2020. Arctic lower-tropospheric warm and cold extremes: horizontal and vertical transport, diabatic processes, and linkage to synoptic circulation features. *J. Clim.* 33 (3), 993–1016. <https://doi.org/10.1175/jcli-d-19-0638.1>.

Peings, Y., 2019. Ural blocking as a driver of early-Winter stratospheric warmings. *Geophys. Res. Lett.* 46 (10), 5460–5468. <https://doi.org/10.1029/2019gl082097>.

Pithan, F., Mauritsen, T., 2014. Arctic amplification dominated by temperature feedbacks in contemporary climate models. *Nat. Geosci.* 7, 181–184. <https://doi.org/10.1038/ngeo20714>.

Polyakov, I.V., Ingvaldsen, R.B., Pnyushkov, A.V., et al., 2023. Fluctuating Atlantic inflows modulate Arctic atlantification. *Science* 381 (6661), 972–979. <https://doi.org/10.1126/science.adh5158>.

Rantanen, M., Karpechko, A.Y., Lipponen, A., Nordling, K., Hyvärinen, O., Ruosteenoja, K., Vihma, T., Laaksonen, A., 2022. The Arctic has warmed nearly four times faster than the globe since 1979. *Commun. Earth Environ.* 3 (1), 168. <https://doi.org/10.1038/s43247-022-00498-3>.

Screen, J.A., Simmonds, I., 2010. The central role of diminishing sea ice in recent Arctic temperature amplification. *Nature* 464 (7293), 1334–1337. <https://doi.org/10.1038/nature09051>.

Screen, J.A., Deser, C., Simmonds, I., 2012. Local and remote controls on observed Arctic warming. *Geophys. Res. Lett.* 39, L10709. <https://doi.org/10.1029/2012GL051598>.

Seager, R., Naik, N., Vecchi, G.A., 2010. Thermodynamic and dynamic mechanisms for large-scale changes in the hydrological cycle in response to global warming. *J. Clim.* 23, 4651–4668. <https://doi.org/10.1175/2010jcli3655.1>.

Serreze, M.C., Barry, R.G., 2011. Processes and impacts of Arctic amplification: a research synthesis. *Glob. Planet. Chang.* 77 (1–2), 85–96. <https://doi.org/10.1016/j.gloplacha.2011.03.004>.

Song, F., Zhang, G.J., Ramanathan, V., Leung, L.R., 2022. Trends in surface equivalent potential temperature: a more comprehensive metric for global warming and weather extremes. *Proc. Natl. Acad. Sci. USA* 119 (6), e2117832119. <https://doi.org/10.1073/pnas.2117832119>.

Tsubouchi, T., Vage, K., Hansen, B., Larsen, K., Osterhus, S., Johnson, C., et al., 2021. Increased ocean heat transport into the Nordic seas and Arctic Ocean over period 1993–2016. *Nat. Clim. Chang.* 11 (1), 21–26. <https://doi.org/10.1038/s41558-020-00941-3>.

Vihma, T., Screen, J., Tjernström, M., Newton, B., Zhang, X., Popova, V., Deser, C., Holland, M., Prowse, T., 2016. The atmospheric role in the Arctic water cycle: a

review on processes, past and future changes, and their impacts. *J. Geophys. Res. Biogeosci.* 121 (3), 586–620. <https://doi.org/10.1002/2015jg003132>.

Wu, B., 2017. Winter atmospheric circulation anomaly associated with recent Arctic Winter warm anomalies. *J. Clim.* 30, 8469–8479. <https://doi.org/10.1175/JCLI-D-17-0175.1>.

Wu, B., Ding, S., 2023. Cold-Eurasia contributes to arctic warm anomalies. *Clim. Dyn.* 60, 4157–4172. <https://doi.org/10.1007/s00382-022-06445-4>.

Wu, B., Wang, J., Walsh, J., 2006. Dipole anomaly in the winter Arctic atmosphere and its association with sea ice motion. *J. Clim.* 19 (2), 210–225. <https://doi.org/10.1175/JCLI3619.1>.

Wu, B., Handorf, D., Dethloff, K., Rinke, A., Hu, A., 2013. Winter weather patterns over Northern Eurasia and Arctic sea ice loss. *Mon. Weather Rev.* 141, 3786–3800. <https://doi.org/10.1175/MWR-D-13-00046.1>.

Wu, Z., Li, X., Li, Y., Li, Y., 2016. Potential influence of Arctic sea ice to the inter-annual variations of East Asian Spring precipitation. *J. Clim.* 29, 2797–2813. <https://doi.org/10.1175/JCLI-D-15-0128.1>.

Wu, G., Ma, T., Liu, Y., Jiang, Z., 2020. PV-Q perspective of cyclogenesis and vertical velocity development downstream of the Tibetan Plateau. *J. Geophys. Res. Atmos.* 125 <https://doi.org/10.1029/2019JD030912> e2019JD030912.

Xie, Y., Huang, J., Ming, Y., 2019. Robust regional warming amplifications directly following the anthropogenic emission. *Earth's Future* 7 (4), 363–369. <https://doi.org/10.1029/2018ef001068>.

Xie, Y., Wu, G., Liu, Y., Huang, J., 2020. Eurasian cooling linked with Arctic warming: insights from PV dynamics. *J. Clim.* 33 (7), 2627–2644. <https://doi.org/10.1175/jcli-d-19-0073.1>.

Xie, Y., Nie, H., He, Y., 2022a. Extratropical climate change during periods before and after an Arctic ice-free summer. *Earth's Future* 10 (8). <https://doi.org/10.1029/2022ef002881> e2022ef002881.

Xie, Y., Wu, G., Liu, Y., Huang, J., Nie, H., 2022b. A dynamic and thermodynamic coupling view of the linkages between Eurasian cooling and Arctic warming. *Clim. Dyn.* 58, 2725–2744. <https://doi.org/10.1007/s00382-021-06029-8>.

Xie, Y., Huang, J., Wu, G., Lei, N., Liu, Y., 2023a. Enhanced Asian warming increases Arctic amplification. *Environ. Res. Lett.* 18 (3), 034041 <https://doi.org/10.1088/1748-9326/acbdb1>.

Xie, Y., Huang, J., Wu, G., Liu, Y., 2023b. Potential vorticity dynamics explain how extratropical oceans and the Arctic modulate wintertime land-temperature variations. *Earth's Future* 11 (2). <https://doi.org/10.1029/2022ef003275>.

Yanai, M., Esbensen, S., Chu, J., 1973. Determination of bulk properties of tropical cloud clusters from large-scale heat and moisture budgets. *J. Atmos. Sci.* 30 (4), 611–627.

Yin, Z., Zhang, Y., Zhou, B., et al., 2023. Subseasonal variability and the Arctic warming-Eurasia cooling trend. *Sci. Bull.* 68, 528–535. <https://doi.org/10.1016/j.scib.2023.02.009>.

You, Q., Cai, Z., Pepin, N., Chen, D., Ahrens, B., Jiang, Z., Wu, F., Kang, S., Zhang, R., Wu, T., Wang, P., Li, M., Zuo, Z., Gao, Y., Zhai, P., Zhang, Y., 2021. Warming amplification over the Arctic Pole and Third Pole: trends, mechanisms and consequences. *Earth Sci. Rev.* 217, 103625 <https://doi.org/10.1016/j.earscirev.2021.103625>.

Zhang, X., Sorteberg, A., Zhang, J., Gerdes, R., Comiso, J.C., 2008. Recent radical shifts of atmospheric circulations and rapid changes in Arctic climate system. *Geophys. Res. Lett.* 35, L22701. <https://doi.org/10.1029/2008GL035607>.

Zhang, X., He, J., Zhang, J., Polyakov, I.V., Gerdes, R., Inoue, J., Wu, P., 2013. Enhanced poleward moisture transport and amplified northern high-latitude wetting trend. *Nat. Clim. Chang.* 3 (1), 47–51. <https://doi.org/10.1038/nclimate1631>.

Zhang, R.N., Zhang, R.H., Dai, G., 2022. Intraseasonal contributions of Arctic sea-ice loss and Pacific decadal oscillation to a century cold event during early 2020/21 winter. *Clim. Dyn.* 58, 741–758. <https://doi.org/10.1007/s00382-021-05931-5>.

Zhang, P., Chen, G., Ting, M., Ruby Leung, L., Guan, B., Li, L., 2023. More frequent atmospheric rivers slow the seasonal recovery of Arctic sea ice. *Nat. Clim. Chang.* 13, 266–273. <https://doi.org/10.1038/s41558-023-01599-3>.